Applied Thermal Engineering 74 (2015) 36–46

Contents lists available at ScienceDirect

Applied Thermal Engineering

journal homepage: www.elsevier.com/locate/apthermeng

A complete transport validated model on a zeolite membrane for carbon dioxide permeance and capture

Evangelos I. Gkanas [a,c,*], Theodore A. Steriotis [b], Athanasios K. Stubos [a], Peter Myler [d], Sofoklis S. Makridis [a,c]

[a] Institute of Nuclear and Radiological Sciences and Technology, Energy and Safety (INRASTES), 'Demokritos', Aghia Paraskevi, 15310 Athens, Greece
[b] Institute of Advanced Materials, Physicochemical Processes, Nanotechnology & Microsystems, NCSR "Demokritos", Aghia Paraskevi, Athens 15310, Greece
[c] Institute for Renewable Energy and Environmental Technologies, University of Bolton, Deane Road, Bolton BL3 5AB, UK
[d] Centre for Advanced Performance Engineering, University of Bolton, Deane Road, Bolton BL3 5AB, UK

GRAPHICAL ABSTRACT

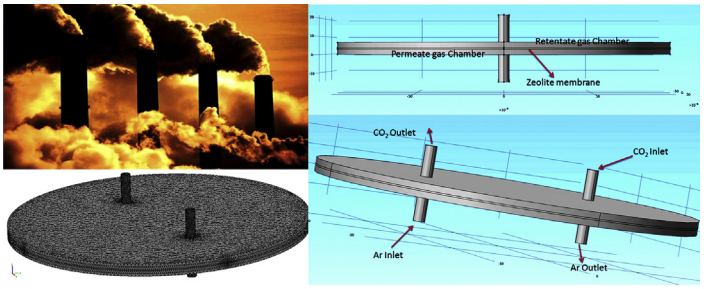

ARTICLE INFO

Article history:
Received 22 August 2013
Accepted 1 February 2014
Available online 1 March 2014

Keywords:
Zeolite membrane
CO_2 permeation
Wicke–Kallenbach cell
Maxwell–Stefan diffusivity
Quasi-chemical approach

ABSTRACT

The CO_2 emissions from major industries can cause serious global environment problems and their mitigation is urgently needed. The use of zeolite membranes is a very efficient way in order to capture CO_2 from some flue gases. Zeolite membranes are porous crystalline materials with pores of a consistent size and these pores are generally of molecular size 0.3 to 1.3 nm, and enable high selectivity and reduced energy requirements in industrial separation applications. Further, zeolites are thermally stable and have known surface properties. Separation in zeolites is mainly based on dissimilarity of diffusivities, favored absorption between the components and/or molecular sieving effects.

The present work is aimed at developing a simulation model for the CO_2 transport through a zeolite membrane and estimate the diffusion phenomenon through a very thin membrane of 150 nm in a Wicke–Kallenbach cell. This apparatus has been modeled with COMSOL Multiphysics software. The gas in the retentate gas chamber is CO_2 and the inert gas is argon. The Maxwell–Stefan surface equations used in order to calculate the velocity gradients inside the zeolite membrane and in order to solve the velocity profile within the permeate and retentate gas chamber, the incompressible Navier–Stokes equations were solved. Finally, the mass balance equation for both gases was solved with the mass balance differential equations. Validation of the model has been obtained at low and high temperatures suggesting that higher the temperature the more beneficial the outcome.

* Corresponding author. Materials, Mechanics and Structures Research Division, Faculty of Engineering, University of Nottingham, Nottingham NG7 2RD, UK.
E-mail addresses: gkanas@ipta.demokritos.gr, egkanas@gmail.com (E.I. Gkanas).

http://dx.doi.org/10.1016/j.applthermaleng.2014.02.006
1359-4311/

Nomenclature

R	gas constant, 8.314 J/mol/K
T	temperature, K
u_i	velocity of species-i with respect to zeolite, m/s
D_{ij}	Maxwell–Stefan diffusivity describing interchange between i and j, m^2/s
D_i	Maxwell–Stefan diffusivity for species i, $m^2\ s^{-1}$
q_i	loading of component i in zeolite, molecules per unit cell or mol kg^{-1}
N_i	molecular flux of species-i, molecules/m^2/s or (mol/m^2/s)
p_i	partial pressure of species-i, Pa
B_{ij}	elements of matrix [B], defined in Eq (10), s/m^2
c	concentration of species, mol/m^3
d	density of CO_2, kg/m^3
n	dynamic viscosity, Pa s
F	volume force, force per unit volume
R	reaction rate, 1/s

Greek letters

μ	chemical potential, J/mol
θ_i	fractional loading of component i, dimensionless
ρ	density of membrane, number of unit cells per m^3 or kg/m^3
Γ_{ij}	elements of the matrix of the thermodynamic correction factor [Γ], dimensionless
∇	gradient operator
∇^2	vector Laplacian
Π	permeance, mol/m^2/s/Pa

Superscripts

sat	referring to saturation loading
s	referring to surface diffusion

1. Introduction

There is a growing consensus among the scientific community that the rising atmospheric levels of CO_2 as a result of human activities, such as emissions from major industries (power generation, steel and cement industries) [1] are that the origin of the warming effect of the climate [2]. Membrane processes appear to be an attractive option to carry out gas separations in terms of their lower environmental impact and energy cost, compared to more conventional separation technologies. Furthermore, the modular nature of membranes constitutes a positive input [3]. Recently, great efforts of novel synthetic routes on membranes for CO_2 removal have been reported [4] mainly based on fabricated cross-linked poly (ethylene-oxide) (PEO) membranes for H_2 purification and CO_2 capture [5] or composite polyetheramine (PEA)–polyhedral oligomeric silsesquioxane (POSS) membranes for CO_2/H_2 and CO_2/N_2 separation [6]. Further, nanohybrid membranes have been investigated with a CO_2/H_2 selectivity of 11 at 35 °C at 3.5 atm [7].

A wide variety of micro- and meso-porous materials are of potential use in separation applications such as CO_2 capture [8–10]. Examples of microporous materials include zeolites (crystalline aluminosilicates) among other materials such as metal–organic frameworks, covalent organic frameworks and zeolitic imidazolate frameworks. Zeolites are inorganic crystalline structures with uniform pores of molecular dimensions. Different pore sizes and composition of zeolites have been used to prepare membranes, and zeolite membranes with different shapes have been investigated to separate CO_2 [11–13]. These materials have unique properties such as a singular pore diameter, well-defined surface properties and high thermal stability making them invaluable in many technical applications [14,15].

In the separation of a mixture by a zeolite membrane the selectivity is a function of the sorption and diffusion and the relevant parameters cannot be simply predicted on the basis of molecular size and shape alone. Key parameters for transport in zeolites by surface and micropore diffusion include temperature, pressure, molecular weight, kinetic molecular diameter, pore diameter, heat of gas adsorption, thermal activation energies for both surface and microporous diffusion. Diffusion is an activated process depending on ΔH_{ads}, on the molecular size of the adsorbate and the fractional coverage [9]. Adsorption is an exothermic, non-activated process which is driven by fugacity. It is a competitive phenomenon [56].

Zeolites can be applied as powders, pellets and as thin films grown on inert support membranes with a larger pore size [16]. In between, numerous zeolite membrane preparations are reported and substantial progress can be stated, examples are the preparations of zeolite membranes of types LTA [17], FAU [18], CHA [9], DDR [20] and mixed tetrahedral–octahedral oxides [21,22]. Since the separation on these membranes is based on competitive adsorption, the selectivities were found to be low. Most often the MFI type membrane was studied [23–25]. Recently, Tsapatsis et al. [26] have prepared *ab*-oriented MFI silicalite-1 membrane, and they further showed the performance of *h*0*h* and *c*-oriented silicalite-1 layers at different temperatures [27,28]. For a silicalite-1 membrane a selectivity of about 10 was obtained [29] and also the CO_2 permeation from pressurized feeds on a silicalite-1 membrane on different supports has been reported [30]. DDR (0.36 nm × 0.44 nm) and SAPO-34 (0.38 nm) have pores that are similar in size to CH_4 (0.34 nm) but larger than CO_2 (33 nm) [9]. It can be expected that these membranes show high CO_2/CH_4 selectivities due to molecular sieving. Very efficient SAPO-34 membranes were synthesized by *in-situ* crystallization on tubular support [31]. It has also been reported that SAPO-34 membranes can separate CO_2 from CH_4 in higher efficiency at lower temperatures with a selectivity of 270 at −20 °C [32]. Recently, the tuning of CO_2 permeation through a SAPO-34 by ion exchange was reported [33,34]. Hasegawa et al. [35] studied Y-type zeolite membranes and found that the membranes synthesized by hydrothermal process on an α-alumina support showed separation factor of CO_2/N_2 149 at 35 °C.

For the applications described above, migration or diffusion of sorption molecules through the pores and cages within the crystal structure of the zeolite membrane is dominant. Configurationally diffusion is the term coined to describe diffusion in zeolites and it is characterized by very small diffusivities (10^{-8} to 10^{-14}) m^2/s [36] with a strong dependence on the size and shape of the quest molecules [37,38] and high activation energy [39]. Further, it is characterized by very strong concentration dependence [40]. The measurement of the diffusivity in zeolites can be obtained by both macroscopic and microscopic methods.

Diffusion of components, especially gases, through porous materials can be experimentally studied with the use of Wicke–Kallenbach (W–K) cells [41,42]. These experimental devices consist of two flow-through components separated by a membrane of porous material through which components can penetrate. A steady gas stream with certain composition flows through the first compartment, while another stream of usually inert gas flows through the second compartment as a sweep gas. Mass transport parameters of component in a porous material are frequently determined from a

transport model developed to explain experimental observations with a W–K cell. Different models have been proposed to describe various transport mechanisms in various inorganic membrane materials [43,44].

Theoretical approaches for modeling the diffusion in zeolites and/or other microporous structures fall into two different categories. A kinetic approach and an approach based on irreversible thermodynamics. The former is based on random walk models and/or transition state theory appropriately modified to account for several additional phenomena such as multilayer adsorption, surface heterogeneity and energy barriers [45–47]. The irreversible thermodynamic approach considers the chemical potential gradient as the driving force for diffusion [48]. Multicomponent interactions occur through competitive equilibrium and/or diffusional sorbate–sorbate interactions. In this case, the driving force exerted on any particular species is balanced by the friction this species experiences with the other species present in the mixture and can be accurately described by the generalized Maxwell–Stefan model for diffusion [49].

In some cases, the membranes can be very thin and in some other cases the membranes can contain large pore cracks and defects. In other cases, permeation flux would be relatively high and if the gas flow rates through the cell are insufficient the component concentration in the Wicke–Kallenbach cell may not be homogeneous. Therefore, a need for a simulation model is essential for the accuracy of the transport parameters obtained from the model. According to the literature, there are several models proposed for the CO_2 capture through zeolite membrane [10,16,19,49,51]. The model is based on the Maxwell–Stefan formulation using a Wicke–Kallenbach cell geometry which is an experimental common geometry but has not been extensively studied by simulation. Perdana et al. [52] presented very nice results. In the current work, a simulation study for CO_2 permeation and capture through a zeolite membrane in a Wicke–Kallenbach geometry has been obtained. A comparison about different scenarios about M–S diffusivity terms has been performed followed by a transient analysis of the permeation. The model was validated with already published experimental results and can be used in order to calculate some crucial parameters such as the M–S terms for some other gases such as N_2 or H_2 which are not clearly defined in the literature.

2. Maxwell–Stefan theory for diffusion through zeolite membranes

The generalized Maxwell–Stefan (GMS) equations have successfully been applied to many systems to describe diffusive transport phenomena in multicomponent mixtures and single component species [50]. These models mainly based on the principle that in order to cause relative motion between individual species in a mixture, a driving force has to be exerted on each of the individual species. This driving force is balanced by the friction these species experiences with the other species in the mixture and the friction between the species and the surface of the membrane. Krishna et al. [50] described the diffusion through the membrane of adsorbed molecules starting from the equation for an n-component mixture:

$$-\nabla\mu_i = RT\sum_{\substack{j=1\\ j\neq i}}^{n}\theta_j\frac{u_i-u_j}{D_{ij}^{s}} + RT\frac{u_i}{D_i^{s}}, \quad i = 1,2,\ldots n \tag{1}$$

where $-\nabla\mu_i$ is the force acting on species i tending to move along the surface with velocity u_i. The first term on the right-hand side describes the friction exerted by adsorbate j on the surface motion of species i, each moving with velocities u_j and u_i with respect to the surface, respectively. The second term deals with the friction between the species i and the surface. D_{ij}^{s} and D_i^{s} represent the corresponding Maxwell–Stefan diffusivities and θ_j is the fractional surface occupancy. The GMS formulation Eq. (1) has been applied successfully to describe transient uptake in zeolites and carbon molecular sieves, and in zeolitic membrane permeation. Generally, a multicomponent Langmuir-type adsorption model is used to describe the fractional occupancies. For thermodynamic consistency, however the saturation loading for all species must be equal in the multicomponent Langmuir model hence the fractional occupancies can be defined as:

$$\theta_i = \frac{q_i}{q^{sat}} \tag{2}$$

According to that fact, for different molecules different amounts are needed to obtain similar levels of fractional occupancies. The fractional occupancies are converted into fluxes using Eq. (3).

$$N_i = \rho q^{sat}\theta_i u_i = \rho q_i u_i \tag{3}$$

In this case, the ideal adsorbed solution (IAS) theory as proposed by Myers and Prausnitz (1965) will be used, which is thermodynamically consistent and can be applied using single component isotherms. Dropping the superscripts for the surface diffusivities in the GMS expression for convenience, multiplication of both sides by θ_i/RT and application of Eq. (2), Eq. (1) can be rewritten as:

$$-\frac{\theta_i}{RT}\nabla\mu_i = \sum_{\substack{j=1\\ j\neq i}}^{n}\theta_i\theta_j\frac{u_i-u_j}{D_{ij}} + \frac{\theta_i u_i}{D_i} = \sum_{\substack{j=1\\ j\neq i}}^{n} q_i q_j\frac{u_i-u_j}{q_i^{sat}q_j^{sat}D_{ij}} + \frac{q_i u_i}{q_i^{sat}D_i} \tag{4}$$

Using the definition of fluxes, Eq. (4) can be written as:

$$-\rho\frac{\theta_i}{RT}\nabla\mu_i = \sum_{\substack{j=1\\ j\neq i}}^{n}\frac{q_j N_i - q_i N_j}{q_i^{sat}q_j^{sat}D_{ij}} + \frac{N_i}{q_i^{sat}D_i}, \quad i = 1,2\ldots n \tag{5}$$

The gradient of the thermodynamic potential can be expressed by terms of thermodynamic factors [47]:

$$-\rho\frac{\theta_i}{RT}\nabla\mu_i = \sum_{j=1}^{n}\Gamma_{ij}\nabla\theta_i, \Gamma_{ij} \equiv \frac{\theta_i}{p_i}\frac{\partial p_i}{\partial\theta_j} \tag{6}$$

where Eq. (6) represents a thermodynamic factor which can be determined by the adsorption isotherm, chosen to relate the surface coverage θ_i to the partial pressure p_i. In the current work the adsorption is described by the extended Langmuir model, Eq. (2).

Eqs. (5) and (6) can be cast in a matrix–vector relation:

$$-\rho[\Gamma](\nabla\theta) = [B]\left[q^{sat}\right]^{-1}(N) \tag{7}$$

where $[q^{sat}]^{-1}$ is a diagonal matrix of saturation loadings and the elements of $[B]$ are given by the following equations:

$$B_{ii} = \frac{1}{D_i} + \sum_{\substack{j=1\\ i\neq j}}^{n}\frac{\theta_i}{D_{ij}} \tag{8}$$

and

$$B_{ij} = -\frac{\theta_j}{D_{ij}} \tag{9}$$

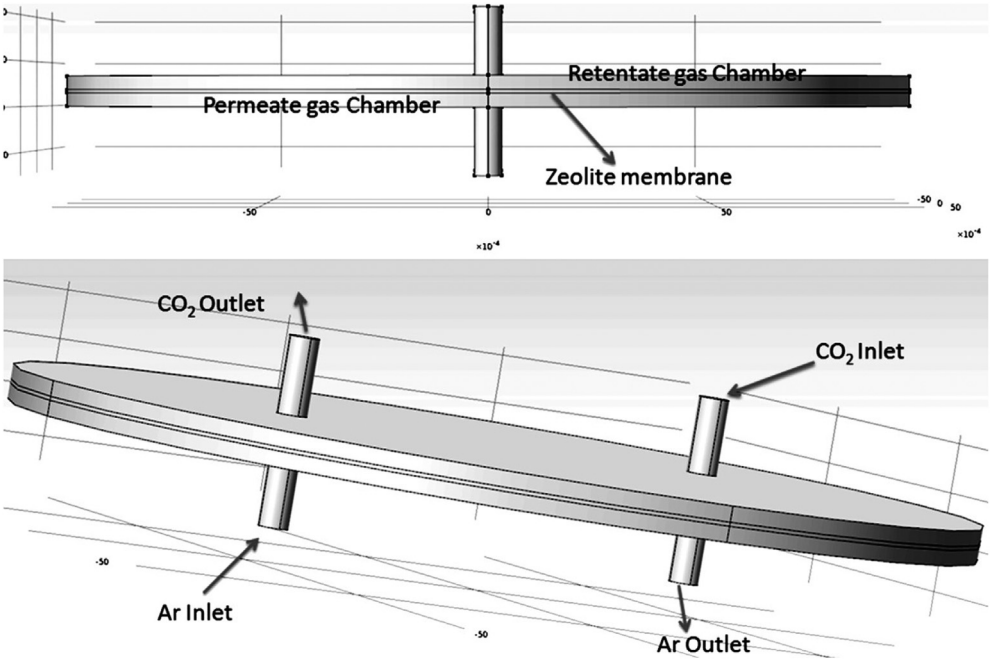

Fig. 1. Geometry of the Wicke–Kallenbach cell.

The solution of Eq. (7) for the diffusion fluxes is the:

$$(N) = -\rho[q^{sat}][B]^{-1}[\Gamma](\nabla\theta) \tag{10}$$

For pure species, which in the current study is CO_2 Eq. (10) can be written as follows:

$$N_i = -\frac{\rho q_i^{sat} D_i \nabla\theta_i}{1-\theta_i} \tag{11}$$

3. Model description

3.1. Geometry of the model

A three-dimensional model has been developed to resolve the flow pattern and CO_2 concentration in the W–K compartment. The development of a three-dimensional model is very important in this case because in the introduction of the partial differential equations describing the CO_2 flux in COMSOL Multiphysics is performed with matrices as already discussed from Eq. (10). With a three-dimensional model a 3×3 matrix describing the CO_2 flux can be used in order to be able to calculate the flux in all the possible directions within the membrane. The zeolite membrane is very thin (approximately 150 nm thick). The cell has cylindrical shape with 19 mm diameter and consist of a retentate gas chamber where the gas CO_2 enters the chamber, and a permeate gas chamber where an inert gas (in this case argon) enters the system. The two chambers are separated by a cylindrical, solid zeolite membrane, usually held within a support system. In order to simplify the current problem some assumptions were taken into account. These assumptions are:

1) The transport of the absorbing components through the zeolite membrane occurs due to surface diffusion, described by the generalized M–S model.
2) Additional contributions such as gas translation are negligible.
3) The pressure drop along each compartment is assumed to be negligible.
4) The deformation of the zeolite membrane under high pressure is negligible.
5) No support layer is taken into account [52].
6) The sweep gas does not experience counter diffusion through the zeolite membrane.

Both gas chambers thickness are 0.3 mm. This counter-current system feeds a concentrated gas-flow into the retentate gas chamber and the chemical species reach the zeolite membrane. A portion of the species diffuses through the zeolite and is removed from the permeate chamber by feeding an inert sweep. The geometry of the model is illustrated in Fig. 1.

The gas flowing in the compartment was modeled using the incompressible Navier–Stokes equations, assuming that the gas flowing in the compartment is in the laminar flow regime. The general equation that defines the incompressible flow is given by:

$$d\frac{\partial u}{\partial t} - n\nabla^2 u + \rho(u\nabla)u + \nabla p = F \tag{12}$$

Furthermore, the mass transport in the compartment is due to both convection and diffusion. The momentum balance equation in the retentate compartment is given by:

$$\frac{\partial c}{\partial t} + \nabla(-D\nabla c) = R - u\nabla c \tag{13}$$

3.2. Boundary conditions

The appropriate boundary conditions for the solution of the problem are described by the following set of equations.

3.2.1. Maxwell–Stefan diffusion through the membrane

The conditions referred to the zeolite membrane domain boundaries, found between permeate and retentate gas chambers are: the Neumann boundary condition which refers to the edges where no flux occurs and the Dirichlet boundary condition, which are used at the interface between the zeolite membrane surface and the respective permeate and retentate gas chambers. The Langmuir isotherm is used in the current study in order to calculate the surface coverage of sites at the interface between the gas

chambers and the solid zeolite membrane. Thus this relationship is defined in the Dirichlet boundary conditions.

3.2.2. Mass balance

The boundary conditions between the gas and the walls of the chamber have been set as:

$$nN = 0,\ N = -D\nabla c + c\vec{u}(\text{Insulation/Symmetry condition}) \quad (14)$$

The boundary condition between the gas and the membrane interface is given by:

$$-D\cdot\nabla c + c\vec{u} = N_0, \quad (15)$$

where N_0 is the inward flux (mol/m^2 s)

4. Results and discussion

4.1. Model verification

In order to validate the model which is proposed in the current study, a comparison between the results extracted from the simulation runs based on the model and experimental results obtained from already published data were performed. As other groups have published their simulation results [51,52] without taking into account the effect of the support resistance on permeation and ultimately analyze the permeation behavior using adsorption and occupancy dependent diffusion within the membrane, in the current study the membrane is treated without support. Himeno et al. [53] measured adsorption isotherms of carbon dioxide at temperatures of 273, 298, 323, 348 K, at a pressure range between 0 and 3500 kPa. In order to compare the simulation results with the experimental data, simulation runs were performed at the same temperatures (273, 298, 323, 348 K). For each temperature, results of CO_2 concentration (mol/kg) obtained for individual pressures with a pressure step of 200 kPa, in order to cover the range of 0–3500 kPa. Finally, the results collected from these simulation runs were compared with the experimental results by Himeno et al. in Fig. 2a. A good agreement between the results is obtained. Further, for lower temperatures, the same process was performed in order to compare the simulation results with the experimental data obtained by van der Bergh et al. [54]. Van der Bergh et al. obtained their results at temperatures of 298, 273, 252 and 195 K in a pressure range between 0 and 100 kPa. Again, for each temperature, simulation runs were performed for pressure steps of 10 kPa to cover the pressure range 0–100 kPa. The comparison of the results is presented in Fig. 2b. According to these data it is obvious that for the temperatures of 298 and 273 K the results of the simulation runs are in good agreement with the experimental data, while for the lower temperatures there is a small deviation between the results, but the shape of the isotherms is almost the same. This could be due to the fact that the support of the membrane might play a major role of thermal insulator at lower temperatures. Further, in order to ensure that the proposed model is able to describe the permeation of CO_2 through every zeolite membrane, a comparison of the simulation performance of three different membranes has been performed with already published experimental results. The three different membranes chosen were: DDR3 zeolite membrane, 5A zeolite membrane and 13X zeolite membrane. For each type of membrane, an adsorption isotherm was measured at constant temperature and compared to experimental data from van den Bergh et al. [54] for the DDR3 membrane,

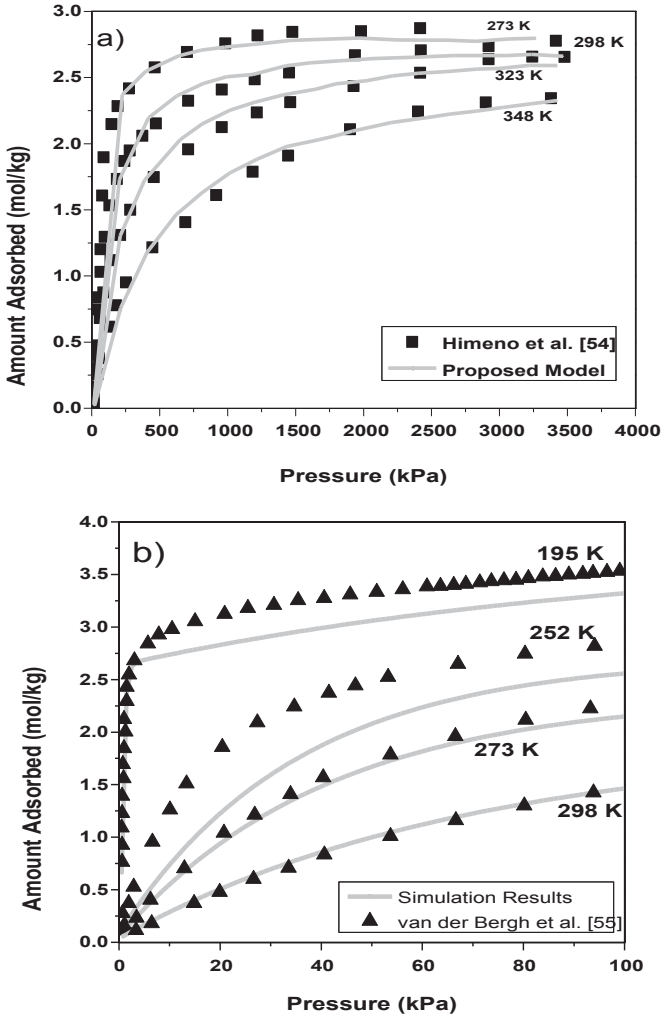

Fig. 2. Comparison of experimental results extracted from recently published adsorption data by Himeno et al. and the simulation results extracted at same temperatures with a pressure step of 200 kPa (a), and experimental adsorption data recently published by van der Bergh et al. and simulation results extracted at same temperatures with a pressure step of 10 kPa (b).

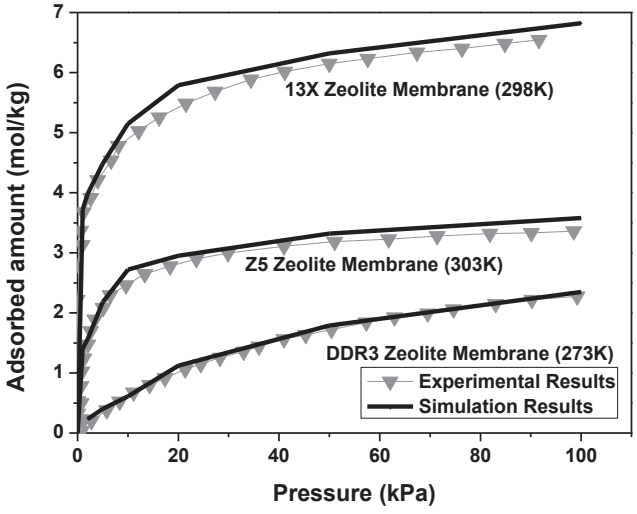

Fig. 3. Comparison of experimental results extracted from recently published adsorption data for three different types of zeolite membranes, DDR3 membrane by van den Bergh et al. [54], Z5 membrane by Liu et al. [2] and 13X membrane by Cavenati et al. [57] and the simulation results extracted at 273 K for the DDR3 membrane, 303 K for the Z5 membrane and 298 K for the 13X membrane.

Liu et al. [2] for the Z5 membrane and Cavenati et al. [57] for the 13X membrane. The temperature for the DDR3 membrane was 273 K, for the Z5 membrane was 303K and for the 13X zeolite membrane 298 K. The results of these measurements are presented in Fig. 3. As extracted from Fig. 3, the data from the simulation runs

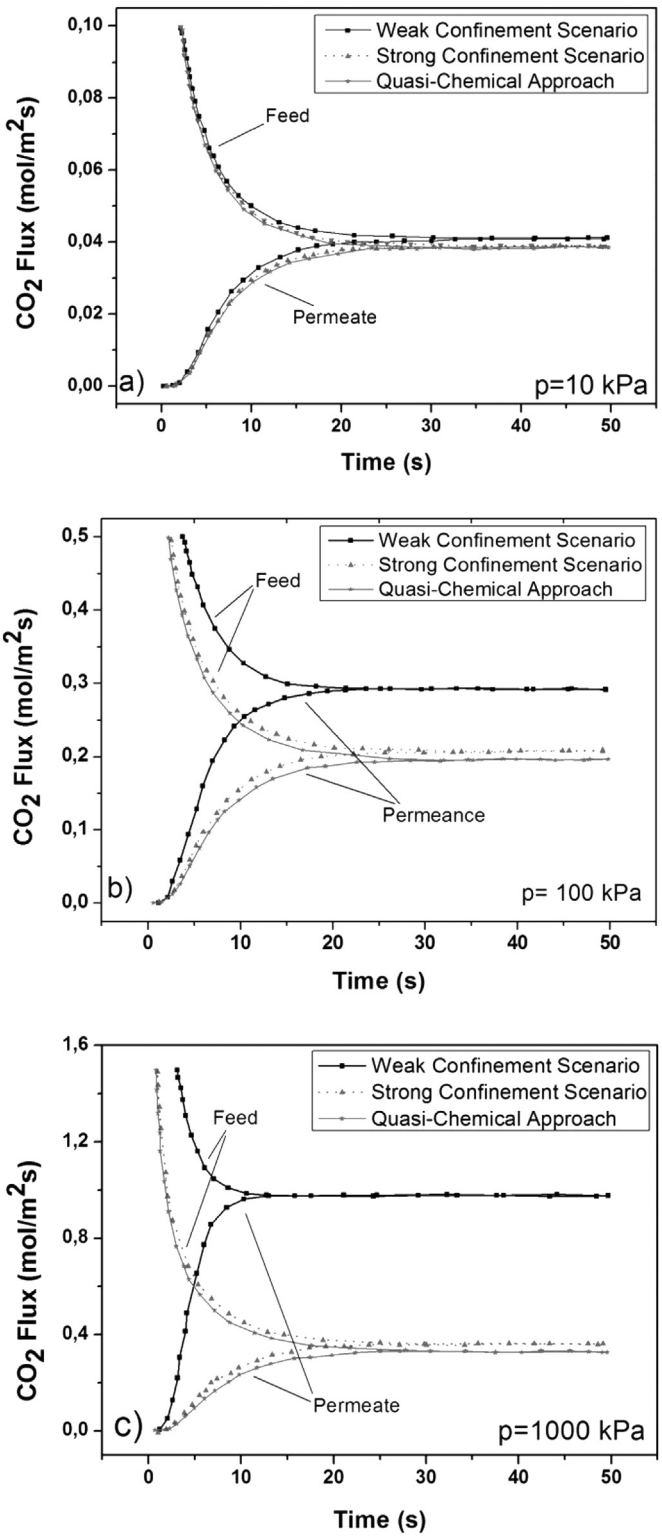

Fig. 4. Transient response to an increase in feed pressure in a CO_2 permeation system. Feed and permeate fluxes for the three different scenarios about the M–S diffusivities for feed pressures a) 10 kPa, b) 100 kPa and c) 1000 kPa.

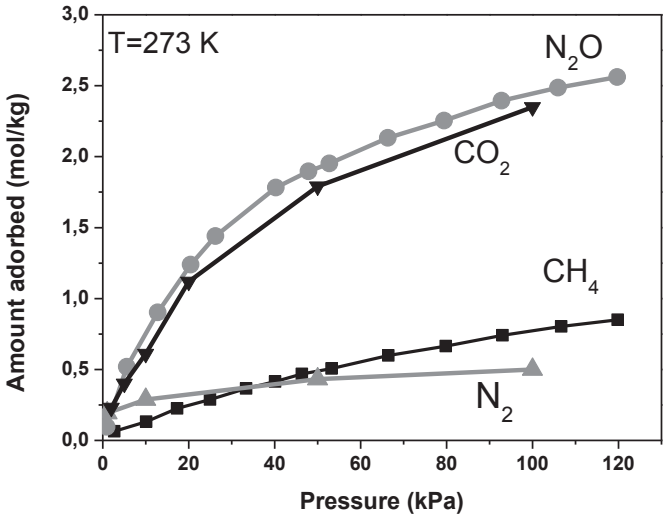

Fig. 5. Adsorption isotherms for carbon dioxide, nitrous oxide, methane and nitrogen in DDR3 zeolite membrane at 273 K.

are in very good agreement with the experimental, indicated that the proposed model is valid for all types of zeolite membranes.

4.2. CO_2 permeation through the zeolite membrane

For single-component diffusion, transport flux of the component through the membrane is described by Eq. (11). The term D_i is referred as M–S surface diffusivity. In the current study, three different M–S diffusivity term scenarios are considered and compared. In the weak confinement scenario the M–S diffusivity acts independently of the fractional occupancy and is equal to the initial zero-loading diffusivity:

$$D_i = D_i(0) \tag{16}$$

In the strong confinement scenario, the M–S diffusivity presents linear dependence on the occupancy:

$$D_i = D_i(0)(1 - \theta_i) \tag{17}$$

Reed and Ehrlich [55] proposed a general occupancy dependence on the M–S diffusivity term:

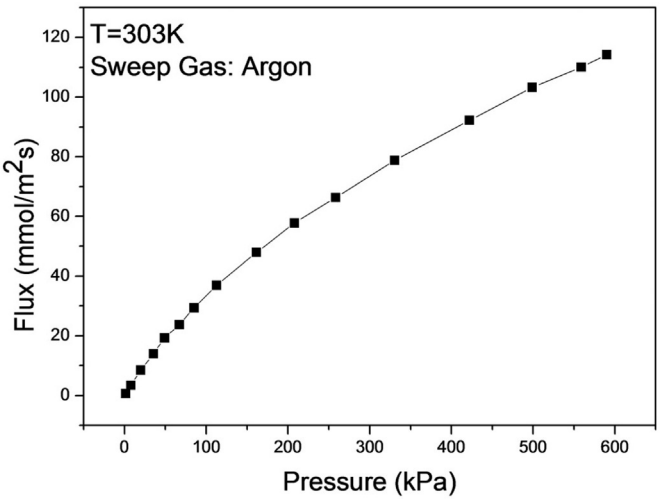

Fig. 6. CO_2 flux as function of the feed pressure at constant temperature 303 K.

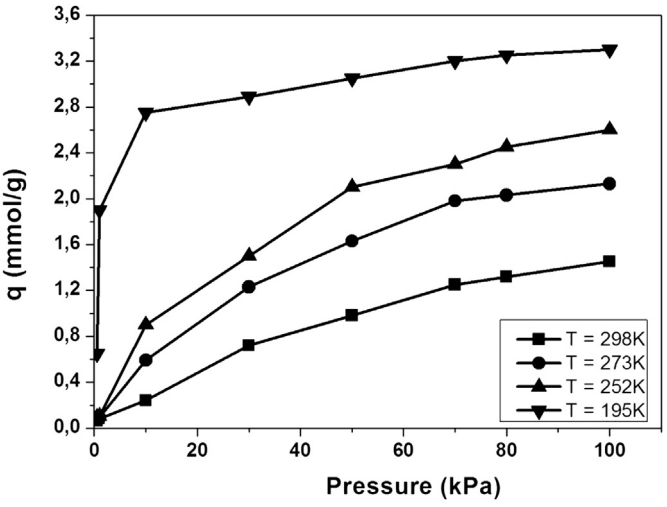

Fig. 7. Adsorption isotherms of carbon dioxide at 195, 252, 273 and 298 K.

Table 1
Langmuir parameters for the temperatures 303, 363 and 423 K.

T (K)	q^{sat} (mol/kg)
303	2.48
363	1.81
423	1.46

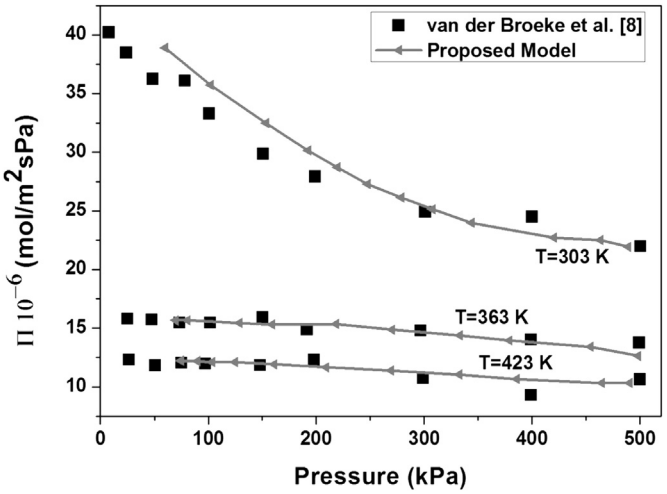

Fig. 9. Comparison of the results extracted from simulation runs and the experimental results extracted from van der Broeke et al. [8] for the effect of pressure and temperature on the permeance.

$$D(\theta) = D(0)\frac{(1+\varepsilon)^{y-1}}{\left(1+\frac{\varepsilon}{f}\right)^{y}} \tag{18}$$

where y is the coordination number (the maximum number of neighbors in the lattice cavity of the membrane) and the other parameters are given by:

$$f = \exp\left(\frac{\delta E}{RT}\right) \tag{19}$$

$$\varepsilon = \frac{(\gamma - 1 + 2\theta)f}{2(1-\theta)} \tag{20}$$

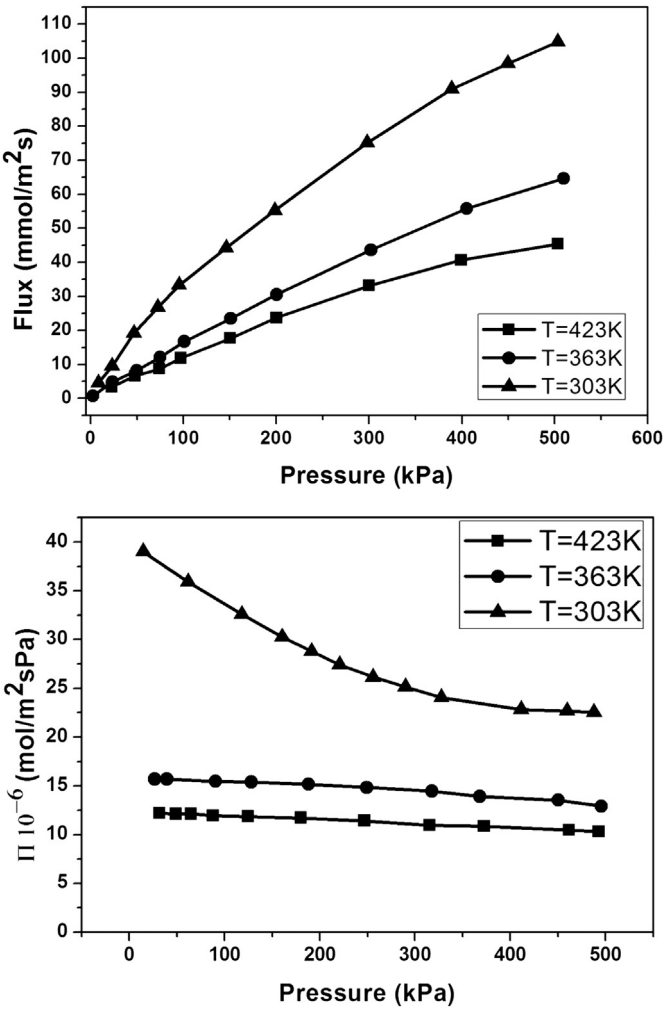

Fig. 8. Effect of pressure and temperature on the permeation of carbon dioxide through the zeolite membrane.

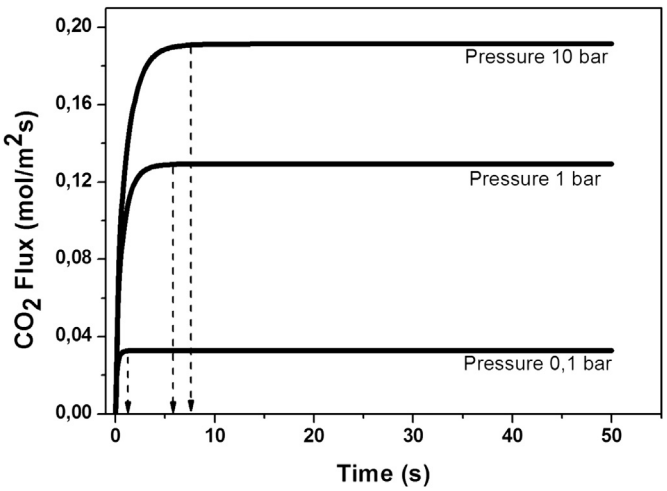

Fig. 10. Transient flux of CO_2 at 303 K for three different feed pressures 10, 100 and 1000 kPa.

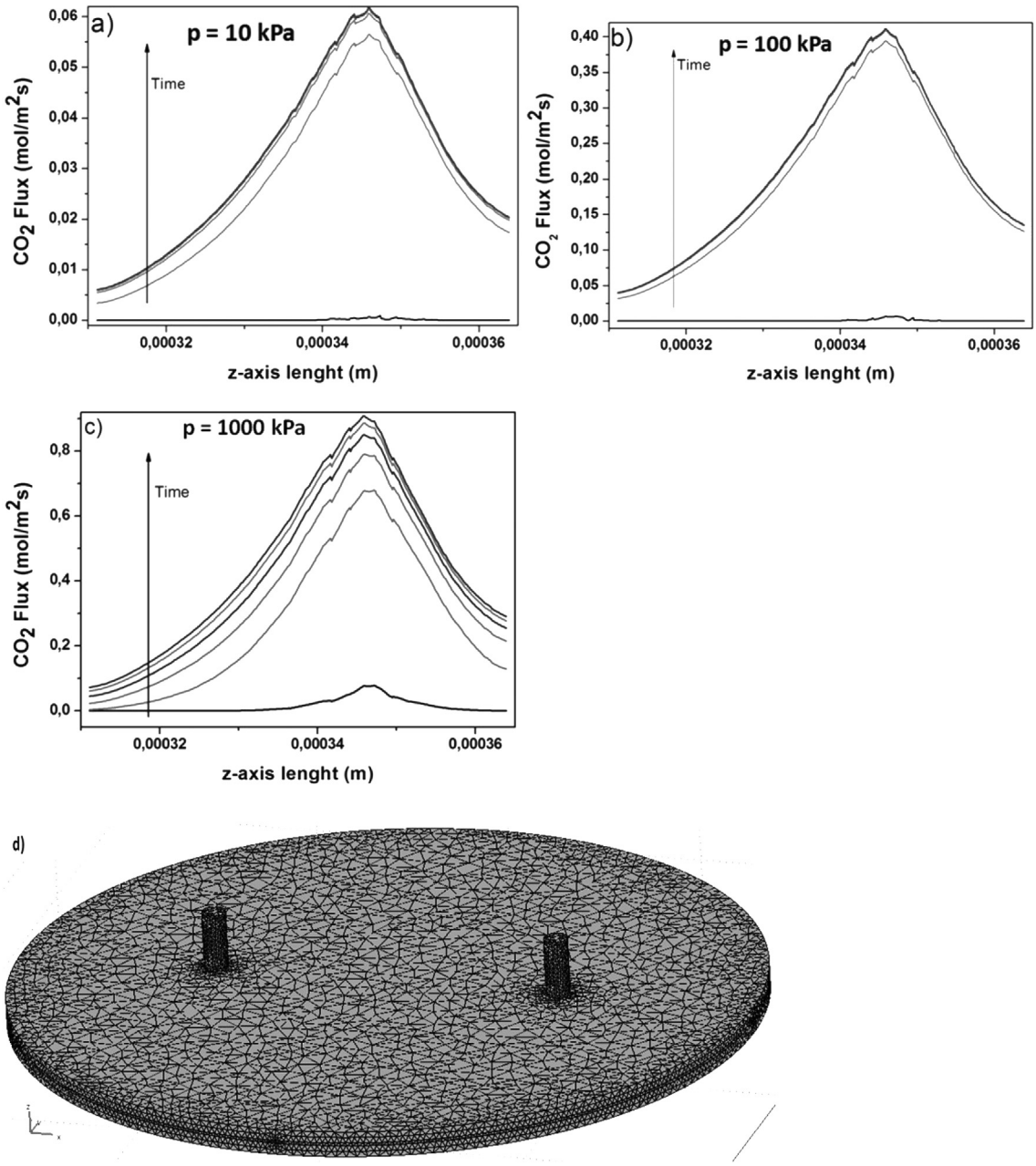

Fig. 11. Transient CO_2 flux analysis across the *z*-axis of the zeolite geometry. Panel a shows the CO_2 flux profile for feed pressure 10 kPa. Panel b shows the CO_2 flux profile for feed pressure 100 kPa. Panel c shows the CO_2 flux profile for feed pressure 1000 kPa and panel d shows the *z*-axis of the zeolite membrane geometry which is the perpendicular axis to the membrane.

$$\gamma = \sqrt{1 - 4\theta(1-\theta)\left(1 - \frac{1}{f}\right)} \tag{21}$$

Fig. 4 shows the transient permeation of pure CO_2 through the zeolite membrane for three different feed pressures (10, 100 and 1000 kPa) and the comparison of the three different M–S diffusivity scenarios described above. All the measurements were performed at temperature 298 K. The fluxes at the feed and the permeate sides are decreasing and increasing respectively until they reach steady state. As the feed pressure increases from 10 to 1000 kPa, there are larger differences among the transient fluxes for the three M–S diffusivity scenarios. However, even at the higher pressure of 1000 kPa the difference between the strong confinement scenario and the quasi-chemical approach is small and this is a consequence of the close diffusivities of CO_2 obtained from these two estimation methods. The same approach was performed by Lee [51] who also pointed that as the feed pressure is increasing, larger differences in the fluxes between the different scenarios are taking place, where the strong confinement scenario with the quasi-chemical approach, have almost the same behavior, even at high pressures. The main difference (which seems to be minor) between the strong confinement scenario and the quasi-chemical approach lies on the fact that the strong confinement scenario depends directly to the fractional occupancy which related with the number of the remaining free spaces for CO_2 capture within the membrane with time, while the quasi-chemical approach depends on more parameters except the occupancy, such as the number of adjacent atoms near the available cavity which might affect the behavior of

the membrane. The weak confinement scenario on the other hand does not takes into account the fractional occupancy indicating that the Maxwell–Stefan diffusivity term remains constant with time. This is probably the main reason that the results extracted from this scenario, doesn't match to the results extracted from the other two scenarios at high pressures. The conclusion of the above results is that in high feed pressures the weak confinement scenario might bring wrong estimated M–S diffusivities while the strong and quasi-chemical approach seems to have better potential in describing the diffusion at higher pressures. At low pressures it seems that all three scenarios can describe with detail the CO_2 diffusion through the zeolite membrane.

The removal of CO_2 is very important for applications such as to purify natural gas, reduce the amount of green gas emission from flue gas and collect methane from landfill gas. Further, industrial gas is a complex mixture containing gaseous hydrocarbons and non-hydrocarbon components. Fig. 5 presents a comparison of the adsorption data for CO_2, CH_4, N_2O and N_2 through a DDR3 zeolite membrane at 273 K for a pressure range from 0 to 100 kPa. The CO_2 and the N_2O isotherms are almost the same and this is something expected because some of the main parameters describing the permeation such as the saturation loading, the adsorption enthalpy, the pro-exponential constant are very close in these two gases. Further, CO_2 and N_2O can be considered as "highly absorbing gases" with respect to the other two gases. The obtained order is the following: $CO_2 \approx N_2O > CH_4 > N_2$.

4.3. Effect of temperature and pressure on the CO_2 permeation through the membrane

The temperature effect on the diffusion through a zeolite membrane is very important and the temperature dependence of the permeance for a large number of gases has been well-studied. Fig. 6, presents the simulation results for the flux of CO_2 through the membrane at a temperature of 303 K and a pressure range from 0 to 600 kPa at temperature 303 K. It is obvious from the results that the flux of CO_2 through the zeolite membrane presents a non-linear dependence on the pressure.

Fig. 7, shows the adsorption isotherm of carbon dioxide in the zeolite membrane at 298, 273, 252 and 195 K for a pressure range from 0 to 100 kPa. It is clearly seen from Fig. 6 that the isotherm changes from a non-linear to an almost linear shape if the temperature is increased. The reason of this behavior will be discussed later.

When the mass transport through the zeolite membrane is described the flux and the permeance are typically used. The permeance is calculated by from a mass balance at steady state by using the pressure difference between the retentate and the permeate side. The permeance can be defined as:

$$\Pi = \frac{N}{\Delta p} \tag{22}$$

where Δp is the pressure difference of CO_2 over the membrane. Sometimes permeance is better quantity to describe the mass transport, because it takes into amount the pressure difference due to some pressure variation problems that might occur due to the sweep gas diffusion mechanism within the membrane. The effect of the isotherm shape on the behavior of the permeation is illustrated in Fig. 8. Panel a presents the CO_2 flux as a function of pressure and panel b the permeance as a function of pressure. The parameters used for these temperatures are presented in Table 1. The simulation results for both the permeance and flux are in great agreement with the experimental results presented by Van der Broeke et al. [12], and the comparison is presented in Fig. 9.

For the lower temperature 303 K both the flux and the permeance present a non-linear behavior on the feed pressure, but this behavior is changing for higher temperatures 363 and 423 K where the permeance for the temperature 423 K is almost constant with pressure. These results are in very good agreement with the equilibrium isotherms that presented in Fig. 7. For an almost linear isotherm the flux shows linear behavior and the permeance seems to be independent of the pressure. This can be explained as follows. The flux through a zeolite membrane is a function of the diffusivity of the component and the amount of the component adsorbed within the zeolite. Diffusion in zeolites is an activated process and the diffusivity increases with the temperature, while the adsorbed amount decreases with the temperature. When decreasing the temperature in zeolite reaches saturation and the decrease of diffusivity begins to dominate due to the asymptotic approach of adsorption saturation.

4.4. Transient analysis of CO_2 permeation through the zeolite membrane

For the transient analysis of the CO_2 permeation through the membrane it is expected that the CO_2 flux through the membrane initially will be increased and after some time the equilibrium situation will achieved. Further, as discussed in Chapter 4.2 the strong confinement scenario was taken into account in order to describe the Maxwell–Stefan diffusivities. Fig. 10 presents the transient flux for CO_2 at temperature 303 K. The feed pressures are 10, 100 and 1000 kPa respectively. From Fig. 10 is extracted that as the feed pressure increases the CO_2 flux also reaches higher levels within the membrane. Further, the equilibrium time is low for all the three pressures ranging from 2 to 7 s and for the lower pressure of 10 kPa it seems that the equilibrium is reached faster than the higher pressures.

Fig. 11 shows the transient profile for CO_2 permeation flux through the membrane across the z-axis of the zeolite membrane geometry which is the perpendicular axis to the membrane as shown in panel d.

The results showed that the flux profile has the same distribution for all the three feed pressures but the flux is higher as the feed pressure increases. The maximum flux value seems to be located in an area higher than the middle of the membrane. This distribution indicates that in the current geometry the flux of the CO_2 through the membrane has a standard profile for all the feed pressures and

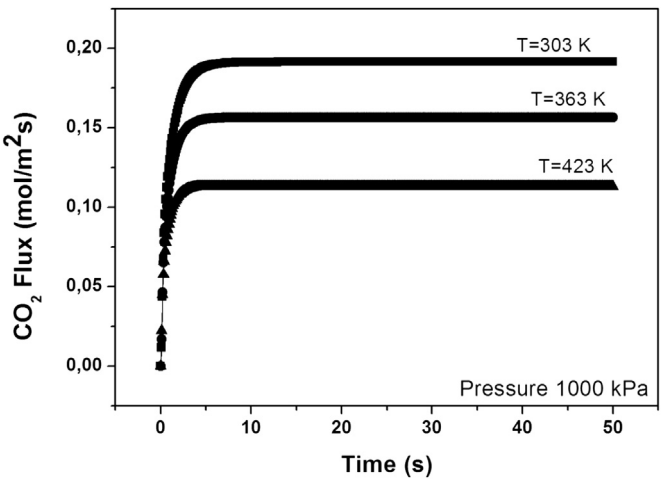

Fig. 12. Transient flux of CO_2 at constant feed pressure 1000 kPa for three different temperatures 303, 363 and 423 K.

according the results of Fig. 10 after some seconds the equilibrium is reached and the flux after the first 7 s is constant.

Fig. 12 shows the transient flux of CO_2 at constant feed pressure 1000 kPa for three different temperatures 303, 363 and 423 K. According to the results extracted from Fig. 12, the CO_2 flux through the membrane is higher for the temperature 303 K and as the temperature increases the flux seems to become lower. Further, it seems that for the lower temperature the equilibrium is reached slower than the case of the higher temperatures.

Fig. 13 presents the transient analysis of the CO_2 flux across the *z*-axis of the zeolite membrane at constant feed pressure 1000 kPa and at three different temperatures 303, 363 and 423 K respectively and these results also indicate that for the current geometry there is a preferred distribution of the CO_2 flux through the membrane. This distribution is presented might due to the way that a Wicke–Kallenbach cell operates.

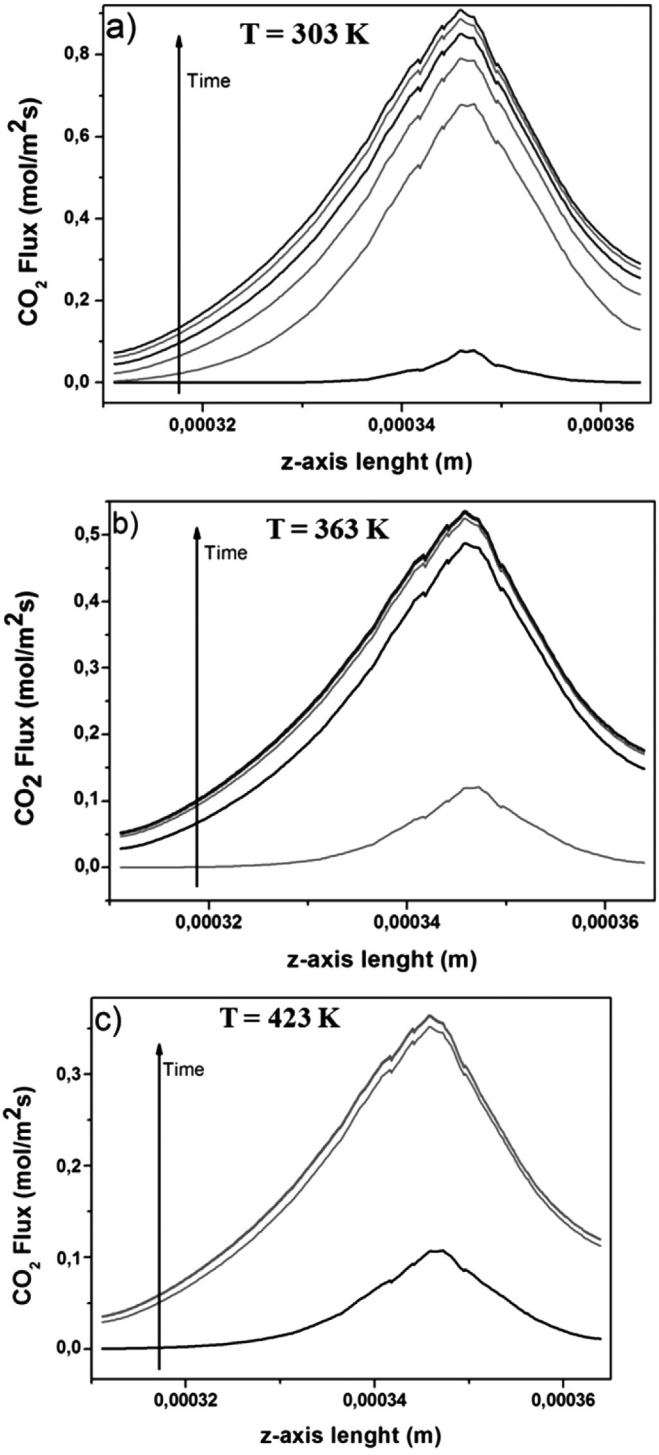

Fig. 13. Transient analysis of the CO_2 flux across the *z*-axis of the zeolite membrane at constant feed pressure 1000 kPa and at three different temperatures 303, 363 and 423 K. Panel a shows the flux for temperature 303 K. Panel b shows the flux for temperature 363 K and panel c shows the flux for temperature 423 K.

5. Conclusions

On the basis of the Maxwell–Stefan approach expressions have been derived for the description of the CO_2 diffusion through the zeolite membrane. A three dimensional study has been performed in a Wicke–Kallenbach cell with diameter of 19 mm successfully indicating a novel approach in this geometry. Argon used as the sweep gas in the permeate gas chamber. The proposed model validated with experimental results and the similarity of the results was satisfying especially at higher temperatures maybe due to the fact that the support of the membrane might play a major role of thermal insulator at lower temperatures. In order to ensure that the proposed model is valid for all zeolitic membranes simulation runs have been performed for three different type of membranes and compared with experimental results. Three different scenarios for the Maxwell–Stefan diffusion term were examined and compared to each other. The results showed that for high supply pressures only the strong and quasi-chemical approach have the potential in describing the CO_2 diffusion. The effect of temperature and pressure in the CO_2 permeation through the membrane was also studied and the results proved that for an almost linear isotherm the flux also can present linear behavior and the permeance is independent of the supply pressure. Finally, the transient analysis showed that the higher the supply pressure the higher the CO_2 flux through the membrane, but for lower pressures the time for reaching equilibrium state is lower. Further, for lower temperatures also the flux is greater comparing to higher temperatures but for the high temperatures the time for reaching equilibrium state is also lower. Finally, a comparison of the permeance behavior of four different gases was studied showed that CO_2 and N_2O are strongly adsorbing gas whereas N_2 and CH_4 are weakly adsorbing gases.

Acknowledgements

The authors are very grateful to Professor Doros N. Theodorou (Head of COMSE Group, Department of Materials Science and Engineering, School of Chemical Engineering, National Technical University of Athens, Greece) for all fruitful discussions on this research work.

References

[1] Stern Review: The Economics of Climate Change, UK Office of Climate Change (OCC), London, 2005. Report available on: http://hm-treasury.gov.uk/sternreview_index.htm.
[2] L. Zhen, C.A. Grande, P. Li, J. Yu, A. Rodrigues, Adsorption and desorption of carbon dioxide and nitrogen on zeolite 5A, Sep. Sci. Technol. 46 (2011) 434–451.
[3] Y.S. Kim, K. Kusakabe, S. Morooka, S.M. Yang, Preparation of microporous silica membranes for gas separation, Korean J. Chem. Eng. 18 (2001) 106–112.
[4] Song Lin Liu, Lu Shao, Mei Ling Chua, Cher Hon Lau, Huan Wang, Shuai Qua, Recent progress in the design of advanced PEO-containing membranes for CO_2 removal, Prog. Polym. Sci. 38 (2013) 1089–1120.
[5] Lu Shao, Shuai Quan, Xi-Quan Cheng, Xiao-Jing Chang, Hong-Guang Sun, Rong-Guo Wang, Developing cross-linked poly(ethylene oxide) membrane by the novel reaction system for H_2 purification, Int. J. Hydrogen Energy 38 (2013) 5122–5132.
[6] Mei Ling Chua, Shao Lu, Bee Ting Low, Youchang Xiao, Tai-Shung Chung, Polyetheramine–polyhedral oligomeric silsesquioxane organic–inorganic

hybrid membranes for CO_2/H_2 and CO_2/N_2 separation, J. Membr. Sci. 385–386 (2011) 40–48.
[7] Cher Hon Lau, Songlin Liu, Donald R. Paul, Jianzhong Xia, Yan-Ching Jean, Hongmin Chen, Shao Lu, Tai-Shung Chung, Silica nanohybrid membranes with high CO_2 affinity for green hydrogen purification, Adv. Energy Mater. 1 (2011) 634–642.
[8] T.C. Merkel, L. Haiqing, W. Xiaotong, R. Baker, Power plant post-combustion carbon dioxide capture: an opportunity for membranes, J. Membr. Sci. 359 (2010) 126–139.
[9] J. Caro, M. Noack, Zeolite membranes–recent developments and progress, Microporous Mesoporous Mater. 115 (2008) 215–233.
[10] R. Krishna, J.M. Van Baten, In silico screening of zeolite membranes for CO_2 capture, J. Membr. Sci. 360 (2010) 323–333.
[11] W. Zhu, P. Hrabanek, L. Gora, F. Kapteijn, J.A. Moulijn, Role of adsorption in the permeation of CH_4 and CO_2 through a silicalite-1 membrane, Ind. Eng. Chem. Res. 45 (2006) 767–772.
[12] Van der Broeke, W.J.W. Baker, F. Kapteijn, J.A. Moulijn, Transport and separation properties of a silicalite-1 membrane—I. Operating conditions, Chem. Eng. Sci. 54 (1999) 245–253.
[13] R. Roque-Malherbe, R. Wendelbo, A. Mifsud, A. Corma, Diffusion of aromatic hydrocarbons in H-ZSM-5, H-Beta, and H-MCM-22 zeolites, J. Phys. Chem. 99 (1995) 14064–14071.
[14] J. Xiao, J. Wei, Diffusion mechanism of hydrocarbons in zeolites—I. Theory, Chem. Eng. Sci. 47 (1992) 1123–1141.
[15] J. Karger, M. Bulow, Theoretical prediction of uptake behaviour in adsorption kinetics of binary gas mixtures using irreversible thermodynamics, Chem. Eng. Sci. 30 (1975) 893–896.
[16] S. Farooq, I.A. Karimi, Modeling support resistance in zeolite membranes modeling, J. Membr. Sci. 186 (2001) 109–121.
[17] M. Lassinantti, J. Hedlund, J. Sterte, Faujasite-type films synthesized by seeding, Microporous Mesoporous Mater. 38 (2000) 25–34.
[18] T. Matsufuji, S. Nakagawa, N. Nishiyam, M. Matsukata, K. Ueyama, Synthesis and permeation studies of ferrierite/alumina composite membranes, Microporous Mesoporous Mater. 38 (2000) 43–50.
[19] H. Lee, P.K. Dutta, Synthesis of free-standing chabazite-type films, Microporous Mesoporous Mater. 38 (2000) 151–159.
[20] T. Tomita, K. Nakayama, H. Sakai, Gas separation characteristics of DDR type zeolite membrane, Microporous Mesoporous Mater. 68 (2004) 71–75.
[21] K.G. Shattuck, B. Yilmaz, J. Warzywoda, A. Sacco, Hydrothermal synthesis of oriented ETS-4 films on porous α-alumina substrates, Microporous Mesoporous Mater. 88 (2006) 56–62.
[22] Z. Lin, J. Rocha, A. Navajas, C. Tellez, J.Q. Coronas, J. Santamaria, Synthesis and characterisation of titanosilicate ETS-10 membranes, Microporous Mesoporous Mater. 67 (2004) 79–84.
[23] C. Algieri, P. Bernardo, G. Golemme, G. Barbieri, E. Drioli, Permeation properties of a thin silicalite-1 (MFI) membrane, J. Membr. Sci. 222 (2003) 181–190.
[24] Y. Takata, T. Tsuru, T. Yoshioka, M. Asaeda, Gas permeation properties of MFI zeolite membranes prepared by the secondary growth of colloidal silicalite and application to the methylation of toluene, Microporous Mesoporous Mater. 54 (2002) 257–268.
[25] T.Q. Gardner, A.I. Flores, R.D. Noble, J.L. Falconer, Measurement of adsorption and diffusion properties of H-ZSM-5 zeolite membranes by a transient Technique, AIChE J. 48 (2002) 1155–1167.
[26] Z. Lai, G. Bonilla, I. Diaz, J.G. Nery, K. Sujaoti, M.A. Amat, E. Kokkoli, O. Terasaki, R.W. Thompson, M. Tsapatsis, D.G. Vlachos, Microstructural optimization of a zeolite membrane for organic vapor separation, Science 100 (2003) 456.
[27] G. Xeromitakis, Z.P. Lai, M. Tsapatsis, Separation of Xylene Isomer Vapors with oriented MFI membranes Made by Seeded growth, Ind. Eng. Chem. Res. 40 (2001) 544–551.
[28] G. Xomeritakis, A. Gouzinis, S. Nair, T. Okubo, M.Y. He, R.M. Overney, M. Tsapatsis, Growth, microstructure, and permeation properties of supported zeolite (MFI) films and membranes prepared by secondary growth, Chem. Eng. Sci. 54 (1999) 3521–3532.
[29] M.C. Lovallo, A. Gouzinis, M. Tsapatsis, Synthesis and characterization of oriented MFI membranes prepared by secondary growth, AIChE J. 44 (1998) 1903–1913.
[30] V. Sebastian, I. Kumakiri, R. Bredesen, M. Menendez, in: Proc. 9th Int. Conf. on Inorganic Membranes, Lillehammer, Norway, 2006, p. 290.
[31] S. Li, J.L. Falconer, R.D. Noble, Improved SAPO-34 membranes for CO_2/CH_4 separations, Adv. Mater. 18 (2006) 2601–2603.
[32] S. Li, J.Q. Martinek, J.L. Falconer, R.D. Noble, T.Q. Gardner, High-pressure CO_2/CH_4 separation using SAPO-34 membranes, Ind. Eng. Chem. Res. 44 (2005) 3220–3228.
[33] M. Hong, S. Li, H.F. Funke, J.L. Falconer, R.D. Noble, Ion-exchanged SAPO-34 membranes for light gas separations, Microporous Mesoporous Mater. 106 (2008) 140–146.
[34] S. Li, J.L. Falconer, R.D. Noble, SAPO-34 membranes for CO_2/CH_4 separation, J. Membr. Sci. 241 (2004) 121–135.
[35] Y. Hasegawa, K. Watanabe, K. Kusakabe, S. Morooka, Influence of alkali cations on permeation properties of Y-type zeolite membranes, J. Membr. Sci. 208 (2002) 415–418.
[36] P.B. Weisz, Zeolites—new horizons in catalysis, Chemtech 3 (1973) 498–505.
[37] J. Wei, A mathematical theory of enchanced paraxylene selectivity in molecular sieve catalysis, J. Catal. 76 (1982) 433–439.
[38] M. Post, Diffusion in zeolite molecular sieves, Surf. Sci. Catal. 58 (1991) 391–443.
[39] D.M. Ruthven, Principles of Adsorption and Adsorption Processes, Wiley, New York, 1984, pp. 124–163.
[40] I.H. Doetch, D.M. Ruthven, K.F. Loughlin, Sorption and diffusion of *n*-heptane in 5A zeolite, Can. J. Chem. 52 (1974) 2717–2724.
[41] P. Capek, V. Hejmanek, O. Solcova, K. Klusacek, P. Schneider, Gas transport in porous media under dynamic conditions, Catal. Today 38 (1997) 31–38.
[42] S.T. Kolaczkowski, Measurement of effective diffusivity in catalyst-coated monoliths, Catal. Today 83 (2003) 85–95.
[43] M.P. Dudukovic, An analytical solution for the transient response in a diffusion cell of the Wicke–Kallenbach type, Chem. Eng. Sci. 37 (1982) 153–158.
[44] O. Solcova, H. Snajdaufova, P. Schneider, Multicomponent counter-current gas diffusion in porous solids: the Graham's law diffusion cell, Chem. Eng. Sci. 56 (2001) 5231–5237.
[45] V.I. Sikavitsas, R.T. Yang, Predicting multicomponent diffusivities for diffusion on surfaces and in molecular sieves with energy heterogeneity, Chem. Eng. Sci. 50 (1995) 3057–3065.
[46] N.C. Karayiannis, V.G. Mavrantzas, D.N. Theodorou, Diffusion of small molecules in disordered media: study of the effect of kinetic and spatial heterogeneities, Chem. Eng. Sci. 56 (2001) 2789–2801.
[47] I.G. Economou, V.E. Raptisa, V.S. Melissasa, D.N. Theodorou, J. Petrou, J.H. Petropoulos, Molecular simulation of structure, thermodynamic and transport properties of polymeric membrane materials for hydrocarbon separation, Fluid Phase Equilib. 228–229 (2005) 15–20.
[48] P. Valertzis, E.S. Kikkinides, M.C. Georgiadis, On the optimization of gas separation processes using zeolite membranes, Trans. IchemE 81 (2003) 525–536.
[49] F. Kapteijn, J.A. Moulijn, R. Krishna, The generalized Maxwell–Stefan model for diffusion in zeolites: sorbate molecules with different saturation loadings, Chem. Eng. Sci. 55 (2000) 2923–2930.
[50] R. Krishna, J.A. Wesselingh, The Maxwell–Stefan approach to mass transfer, Chem. Eng. Sci. 52 (1997) 861–911.
[51] S.C. Lee, Prediction of permeation behavior of CO_2 and CH_4 through silicalite-1 membranes in single-component or binary mixture systems using occupancy-dependent Maxwell–Stefan diffusivities, J. Membr. Sci. 306 (2007) 267–276.
[52] I. Perdana, B.W. Tyoso, I.M. Berdiyasa, S.K. Wirawan, D. Creaser, Effect of external mass transport on permeation in a Wicke–Kallenbach cell, Chem. Eng. Res. Des. 87 (2009) 1438–1447.
[53] S. Himeno, T. Tomita, K. Suzuki, S. Yoshida, Characterization and selectivity for methane and carbon dioxide adsorption on the all-silica DD3R zeolite, Microporous Mesoporous Mater. 98 (2007) 62–69.
[54] J. van den Bergh, W. Zhu, J. Gascon, J.A. Moulijn, F. Kapteijn, Separation and permeation characteristics of a DD3R zeolite membrane, J. Membr. Sci. 316 (2008) 35–45.
[55] D.A. Reed, G. Ehrlichm, Surface diffusion, atomic jump rates and thermodynamics, Surf. Sci. 102 (1981) 588.
[56] J. Caro, M. Noack, P. Kölsch, R. Schäfer, Zeolite membranes – state of their development and perspective, Microporous Mesoporous Mater. 38 (2000) 3–24.
[57] S. Cavenati, C.A. Grande, A.E. Rodrigues, Adsorption equilibrium of methane, carbon dioxide and nitrogen on zeolite 13X at high pressures, J. Chem. Eng. Data 49 (2004) 1095–1101.